

DIPARTIMENTO DI MATEMATICA
POLITECNICO DI MILANO

**A Graph Theoretical Approach to Neurobiological
Databases Comparison**

Dulio, P.; Finotelli, P.

Collezione dei *Quaderni di Dipartimento*, numero **QDD 214**
Inserito negli *Archivi Digitali di Dipartimento* in data 14-10-2015



Piazza Leonardo da Vinci, 32 - 20133 Milano (Italy)

A Graph-Theoretical Approach to Neurobiological Databases Comparison

P. Finotelli^{a,*}, P. Dulio^a, F. Panzica^b, G. Varotto^b, F. Rotondi^b

^a*Dipartimento di Matematica "F. Brioschi", Politecnico di Milano,
Piazza Leonardo da Vinci 32, I-20133 Milano*

^b*Carlo Besta Neurological Institute, Via G. Celoria 11, I-20133 Milano*

Abstract

Music is one of the best tools to evoke emotions and feelings in people. Generally, people like classical music, R&B, hip hop, house, disco, underground or other kinds of music. People select songs basing on their preferences. For example, a subject while performing an action such as running, studying or relaxing tends to listen to songs that give her/him a pleasant feeling. Interesting issues emerge: First, collecting the brain reactions when the brain is stimulated by songs (classified as pleasant). Second, comparing them with the resting state condition, and third representing the neural network changes in terms of emergent subgraphs. We propose a general methodology concerning phase transitions analysis of an arbitrary number of conditions. We also apply such a methodology to real acoustic data and, though our findings generally seem to agree with others available in the literature, they also point out the existence of functional connectivity between pairs of cerebral areas, usually not immediately associated to an acoustical task. Our results may explain why people when listening to pleasant music activated emotional cerebral areas in spite of the fact that the music they classify as pleasant is different for each subject. Possible applications to Neuropsychiatry are discussed.

Keywords: Brain networks, Connectome, Functional matrix, MEG data, Graphs

1. Introduction

In this paper we suggest a possible approach to neurobiological databases management. Data are organized in matrices that, at a later stage, are compressed and compared in a complete way. The problem of thresholding is fully described and detailed. In order to model the neurobiological phenomenon into binary matrices and consequently in terms of graphs. Hence, it results the graph representation of the neurobiological test. From the general graph we can extract suitable subgraphs showing the links that are more involved, to some extent, in the performance. Importantly, our methodology applies to a wealth of datasets which are typically gathered in human subjects by non-invasive methods, such as EEG/MEG [17], fMRI [13], PET [12] or a coupling of an electrophysiologic measurement technique with a hemodynamic one.

This could help to identify the regions responsible for psychiatric disorders, as well as to assess how different tasks of different nature (musical, cognitive, decisional-making, etc.) affect the functional connectivity of the brain.

*Corresponding author

Email addresses: paolo.finotelli@polimi.it (P. Finotelli), paolo.dulio@polimi.it (P. Dulio), Ferruccio.Panzica@istituto-besta.it (F. Panzica), Giulia.Varotto@istituto-besta.it (G. Varotto), Fabio.Rotondi@istituto-besta.it (F. Rotondi)

As an example we provide the application of our proposal to real MEG data (released by Carlo Besta Neurological Institute), concerning two different subjects undergoing the same acoustical experiment.

We investigated the changes in the functional connectivity produced by transitions from *Basal* to *Pleasant*, due to musical experiments. More precisely, two healthy volunteers (in the following referred to as *Abbondanza* and *Bologna*) were considered, and studied under two different states. The first state, the Basal condition, or Basal phase, consisted in a kind of resting state (which can be assumed as a sort of baseline), and was determined when no kind of music was proposed to the volunteers. The second state was a pleasant condition, called the Pleasant phase, obtained while playing a piece of music that, according to some parameters fixed in advance, was considered pleasant to the volunteers (not necessarily the same kind of music was considered pleasant by the subjects).

Both the subjects were investigated by means of MEG technique which model the neural brain network as a graph consisting of 89 nodes (cf. Table 1). The experiments had a duration of 60 seconds in each one of the two considered conditions (Basal and Pleasant).

For every volunteer, the corresponding Basal and Pleasant databases, were collected. This was done by splitting the length of the musical stimulus, which is 60 seconds, in 30 slots of 2 seconds, and recording, in any single slot, the functional connectivity between any pair of nodes. For the sake of precision, in the experiment were considered only 29 slots. In fact, having left out from the analysis the first and the last milliseconds of the stimulus, 29 were the remaining slots, each lasting two seconds.

This resulted in 29×2 different 89×89 -sized matrices $A_t^{(s)} = [a_{hk}]_t^{(s)}$, $1 \leq h, k \leq 89$, $0 \leq t \leq 29$, and $s = 1, 2$ corresponding to the Basal and Pleasant conditions, respectively. For each fixed t and s , the entry a_{hk} of $A_t^{(s)}$ denotes the functional connectivity between the nodes h and k , at the fixed time t , and in the fixed state s . As a consequence, the range of the entries is the $[0, 1]$ real interval. In fact, the functional connectivity is assumed to be symmetric, namely $a_{hk} = a_{kh}$ for all $h, k \in \{1, \dots, 89\}$, and consequently, in order to reduce the data storage, each matrix $A_t^{(s)}$, $1 \leq t \leq 29$, $s = 1, 2$, was available in its upper-triangular form, where $a_{hk} = 0$ for all $h \geq k$.

In Section 2 we detail the general approach that we propose to follow when studying the comparison between different homogeneous databases.

Section 3 shows how the proposed methodology can be applied, giving all details and global comments and remarks. In Subsections 3.6.1, 3.6.2 we provide an example of graph theoretical approach to real data. Emphasis is given to the role of the weights of the edges which, in some sense, play a fundamental role in determining which links are more important in comparison to others in an emergent subgraph.

The results are shown in Section 4 while in Section 5 we resume our conclusions and outline possible extension of our work.

2. Mathematical methodology for thresholding

2.1. Statistical approach

Let us to suppose to perform a neurobiological experiment, whose temporal length is T . Generally, in order to process data, T is split in N temporal sub-intervals, also known as *temporal slots* or *epochs*.

Very often, in neurobiological experiments, data are collected in matrices whose dimensions depend on the number of nodes (denoted by n) and on the number of temporal sub-intervals. Hence, we should speak about a collection of matrices rather than a single matrix. Such a general collection is composed by N matrices of n row and n columns, said differently the dimension of each of these N matrices is $n \times n$. Therefore, every temporal slot is characterized by functional data collected in the form of a $n \times n$ matrix. This holds for each one of the s subjects under

Nodes and correspondent cerebral areas

Node	Cerebral area	Node	Cerebral area	Node	Cerebral area
1	Left Amygdala	31	Right medial frontal gyrus	61	Left Superior parietal lobule
2	Right Amygdala	32	Left superior frontal gyrus, orbital part	62	Right Superior parietal lobule
3	Left Angular Gyrus	33	Right superior frontal gyrus, orbital part	63	Left Postcentral gyrus
4	Angular Gyrus	34	Right superior frontal gyrus	64	Right Postcentral gyrus
5	Left calcarine sulcus (or left calcarine fissure)	35	Left fusiform gyrus	65	Left precentral gyrus
6	Right calcarine sulcus (or right calcarine fissure)	36	Right fusiform gyrus	66	Right precentral gyrus
7	Left Caudate nucleus	37	Left Heschl's gyrus or Left transverse temporal gyrus	67	Left Precuneus
8	Right Caudate nucleus	38	Right Heschl's gyrus or Right transverse temporal gyrus	68	Right Precuneus
9	Left Anterior cingulum	39	Left Hippocampus	69	Right Putamen
10	Right Anterior cingulum	40	Right Hippocampus	70	Right Putamen
11	Left Middle cingulum.	41	Left Insula	71	Left Putamen
12	Right Middle cingulum.	42	Right Insula	72	Right gyrus rectus
13	Left Posterior cingulum	43	Left Lingual gyrus	73	Left Rolandic operculum
14	Right Posterior cingulum	44	Right Lingual gyrus	74	Right Rolandic operculum
15	Left Cuneus	45	Left inferior occipital gyrus	75	Left supplementary motor area
16	Right Cuneus	46	Right inferior occipital gyrus	76	Right supplementary motor area
17	Left inferior frontal gyrus, opercular part	47	Left middle occipital gyrus	77	Left supramarginal gyrus
18	Right inferior frontal gyrus, opercular part	48	Right middle occipital gyrus	78	Right supramarginal gyrus
19	Left inferior frontal gyrus, orbital part	49	Left superior occipital gyrus	79	Left inferior temporal gyrus
20	Right inferior frontal gyrus, orbital part	50	Right superior occipital gyrus	80	Right inferior temporal gyrus
21	Left inferior frontal gyrus, triangular part	51	Left olfactory cortex	81	Left middle temporal gyrus
22	Right inferior frontal gyrus, triangular part	52	Right olfactory cortex	82	Right middle temporal gyrus
23	Left medial orbitofrontal cortex	53	Left globus pallidus	83	Left middle temporal pole
24	Right medial orbitofrontal cortex	54	Right globus pallidus	84	Right middle temporal pole
25	Left middle frontal gyrus	55	Left parahippocampal gyrus	85	Left superior temporal pole
26	Right middle frontal gyrus, orbital part	56	Right parahippocampal gyrus	86	Right superior temporal pole
27	Left middle frontal gyrus, orbital part	57	Left paracentral lobule	87	Left superior temporal gyrus
28	Right middle frontal gyrus	58	Right paracentral lobule	88	Right superior temporal gyrus
29	Left superior frontal gyrus	59	Left inferior parietal lobule	89	Left Thalamus
30	Right superior frontal gyrus	60	Right inferior parietal lobule		

Table 1: Brain atlas.

investigation.

The first step in the analysis consists in importing the available $N \times s$ different upper-triangular $n \times n$ -sized matrices $A_t^{(s)}$ as *Matlab*[®] files (or as other technical computing languages such as *Mathematica*[®]).

Functional brain connectivity forms a full symmetric matrix. It is well known [13], [14], [16], [19] that each entry encodes statistical dependence between two neural elements, which can be cerebral areas or part of them. Such neural elements are associated to voxels. Differently, in case of effective connectivity the matrix is typically skew symmetric. For simplicity we focus on functional connectivity, so we consider symmetric matrices.

In order to save space the storage of real data could be confined in the upper (or lower) triangular part of the matrix. Then, to get a properly symmetric form, which allows a better managing of the *Matlab*[®] scripts, each matrix is added to its transposed, so to obtain symmetric matrices. Of course, the resulting symmetric matrices have zero entries on the main diagonal, which represents the absence of self loops in the neural brain network, meaning that nodes autocorrelation is excluded. Moreover, each entry should be rounded at some decimal digit, depending on the demanded precision.

The comparison between two different states should be managed by computing the differences of the elements belonging to the corresponding databases.

A main problem in the analysis could be caused by the fact that each one of s available databases has no temporal correlation with the others. This means that, for a fixed index $t \in \{1, \dots, N\}$, the matrix $A_t^{(s)}$ refers to different temporal slots for different values of s . As a consequence, a precise picture of the transition from one state to the other requires a kind of randomization. This is obtained by computing all the possible differences between pairs of matrices belonging to the two related databases.

In detail, it should be fixed one matrix corresponding to a particular phase $A_i^{(\bar{s})}$, with \bar{s} and \bar{i} fixed, this means that we consider a particular phase s and a specific temporal slot i . This matrix should be cross-confronted with all the N matrices corresponding to the other phases. In this way we get matrices of the type: $A_i^{(\bar{s})} - A_i^{(s)}$, with $\bar{s} \neq s$. We remark that the phase \bar{s} is fixed and compared to the other phases (that we generally denote with s)

The operation should be repeated for any temporal slot and for any phase (of course it does not considered the confrontation of a phase with itself). For example if two phases, \bar{s} and \tilde{s} are considered then the randomization would create a cell of order $N \times N$ made up of matrices whose dimension is $n \times n$. In case of a third phase \hat{s} is considered, then it is necessary to compare all the possible pairs of available databases.

In order to streamline our description, let us consider two conditions \bar{s} and \tilde{s} . To this step, great importance is assumed by entries of the matrices $A_i^{(\bar{s})} - A_j^{(\tilde{s})}$, $i, j \in 1, \dots, N$, with i fixed time by time, and with \bar{s} and \tilde{s} representing two different phases. In particular, attention should be focused on the entries having smaller or greater absolute values, because they denote the greater agreement or differences in correlations. Since the range of the entries is $[-1, 1]$ one should be mainly interested to center the focus on a right neighborhood of -1 , on a left neighborhood of $+1$, and on the neighborhood of 0 . The width of these neighborhood depending on the distribution of the entries of each matrix. The right neighborhood of -1 represents the situation where the phase \tilde{s} dominate the phase \bar{s} , while left neighborhood of $+1$ refers to the case in where the phase \bar{s} prevails on the phase \tilde{s} . The neighborhood of 0 gives information about the invariance domain between the phase \bar{s} and \tilde{s} .

With the purpose to analyze the entries of the matrices $A_i^{(\bar{s})} - A_j^{(\tilde{s})}$, we organized each column, or equivalently each temporal slot, in a single $n \times n \cdot N$ -sized matrix $C_i = [c_{hi}]_i$ ($i \in \{1, \dots, N\}$, $h \in$

$\{1, \dots, n\}, l \in \{1, \dots, n \cdot N\}$), obtained by connecting the rows of all the N matrices $A_i^{(s)} - A_j^{(s)}$, $i, j \in 1, \dots, N$ of size $n \times n$ forming the column, see (1).

In summary, for each column, that is related to a temporal slot, a single matrix made up of side by side placing of N matrices whose dimension is $n \times n$ is obtained. For example, for the first temporal slot, the matrices $A_1^{(s)} - A_1^{(s)}, A_1^{(s)} - A_2^{(s)}, \dots, A_1^{(s)} - A_N^{(s)}$ must be side by side placed in order to get one single matrix $C_1 = [c_{hl}]_1$ ($h \in \{1, \dots, n\}, l \in \{1, \dots, n \cdot N\}$). Similarly for the other temporal slots. At the end of this process N matrices $C_1 = [c_{hl}]_1, C_2 = [c_{hl}]_2, \dots, C_N = [c_{hl}]_N$, where $h \in \{1, \dots, n\}, l \in \{1, \dots, n \cdot N\}$, are generated.

$$C_i = [A_i^{(s)} - A_1^{(s)} \mid A_i^{(s)} - A_2^{(s)} \mid \dots \mid A_i^{(s)} - A_N^{(s)}], \quad \forall i = 1, \dots, N. \quad (1)$$

Once such matrices are obtained, an analysis on their entries is demanded. The entries of every matrix $C_i = [c_{hl}]_i$ ($i \in \{1, \dots, N\}, h \in \{1, \dots, n\}, l \in \{1, \dots, n \cdot N\}$), are collected in a single array. This is done by concatenating together the N rows of $C_i = [c_{hl}]_i$. This means that N arrays, each one composed by $n \times N \times n$ elements, are generated. This operation is needed to start the statistical analysis.

As a next step, the distribution of the entries of every array should be computed and organized in an histogram formed by a number of bins, each bin representing the frequency of the corresponding entry. A typical histogram of such a type is shown if Figure 1.

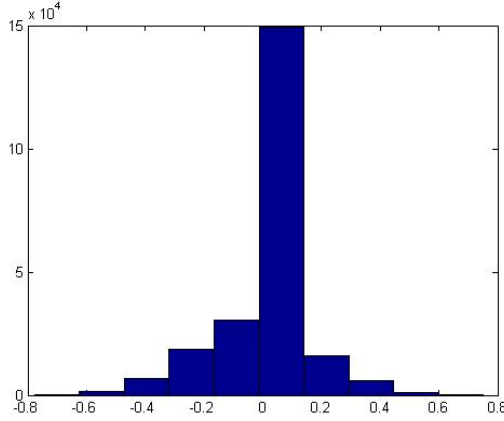


Figure 1: A typical histogram representing the frequency of the entries of matrix C_i , i.e. the distribution of the values of the entries of C_i , $i = 1, \dots, N$.

This is useful in order to focus on the regions of interest which are mainly related to the goal of the experiments.

For example, if one is interested in detecting the links that are invariant under a transition the focus should be on the bin which contains the zero entries. On the contrary, if the goal of the experiment is to find the links which are steadily different throughout the experiment, then the attention should be directed to the bins lying in suitable neighborhoods of -1 and $+1$ which represent the higher possible differences.

2.2. Thresholding towards a graph representation

In order to give a graph representation of the comparison, the matrices related to every temporal slot should be thresholded to yield binary symmetric matrices.

At this step it is possible to perform an analysis to establish suitable thresholds. In fact, due to the amount of data, the matrices related to every temporal slot should be thresholded with the purpose to yield binary symmetric matrices or equivalently undirected graphs [18]. Basically, thresholding may be interpreted as a control of the degree of sparsity [16], [19].

A possible choice to select the thresholds (or the thresholds) is to refer to the center (centers) of the selected bin (bins).

As concerns the neighborhood of -1 , we propose the threshold $\xi_i(L)$, corresponding for each $i \in 1, \dots, N$, to the center of the yielded bin in the histogram related to the slot i . L stands for left part of the histogram.

Therefore, for each $i \in 1, \dots, N$, the matrix $C_i = [c_{hl}]_i$ is thresholded and turned into a binary matrix $[C_i]_L^- = [\tilde{c}_{hl}^i]$, where

$$\tilde{c}_{hl}^i = \begin{cases} 1 & \text{if } c_{hl}^i \leq \xi_i(L), \\ 0 & \text{otherwise.} \end{cases}$$

Analogously, for a neighborhood of $+1$ we fix a threshold $\xi_i(R)$ determining the left neighborhood of $+1$, to get $[C_i]_R^+ = [\tilde{c}_{hl}^i]$, where

$$\tilde{c}_{hl}^i = \begin{cases} 1 & \text{if } c_{hl}^i \geq \xi_i(R), \\ 0 & \text{otherwise.} \end{cases}$$

For each $i = 1, \dots, N$, the corresponding N left thresholded $n \times n$ -sized binary matrices should be summed up to form a matrix $S_i(L)$ that condenses the information in the right neighborhood of -1 . Each entry of $S_i(L)$ ranges from 0 to N , which denotes the number of slots of $\frac{T}{N}$ seconds where the corresponding pair of nodes are correlated. Analogously, a matrix $S_i(R)$, where the information in the left neighborhood of 1 are condensed, is obtained.

From these matrices several types of graphs can be derived that could be assumed as representative of the transition between a phase \bar{s} and \tilde{s} . These could be obtained by fixing a new threshold λ , $\lambda \in \{1, 2, \dots, N\}$, corresponding to the minimum number of slots of $\frac{T}{N}$ seconds that we assumed as indicative of a permanent difference between the \bar{s} and the \tilde{s} states. Of course $\lambda = N$ denotes an absolute permanent difference, and represents a theoretical threshold. More realistically, we should relax this threshold to some intermediate value.

Following the above argument, it is advisable firstly computing the effective maximum M_i of each matrix $S_i(L)$ and investigate the cases where λ concerns some percentage of M_i , such as $\lambda = \frac{4}{5} M_i$, corresponding to the 80% of the slots, or $\lambda = \frac{1}{2} M_i$, namely, the 50% of the slots.

2.3. Graph theoretical approach

Then, a graph theoretical analysis can be outlined, which gives a wealth of information on brain networks.

From a mathematical point of view Theory of Graphs [5] is used to model the brain, seen as a complex network [4], [6], [9], [16], [19]. Firstly, nodes and edges must be fixed, and the architecture of the network must be established. Usually it corresponds to a small-world organization, i.e. an architecture between a totally ordered and a totally random structure. Then, it needs to understand the main relationships existing between nodes and edges. For example, it becomes important to understand how “central” is the role played by a node in a graph, if nodes tend to cluster together, how much the nodes are “interconnected” (this is fundamental for the transfer of information in the brain network). Further lines of research concern the investigation of the mutual node distances (meaning the discrete distance or the Euclidean one) which enlightens how groups of nodes (i.e. mesoscopic structures) communicate.

Moreover, Theory of Graph is also employed in modeling brain disorders [1], [11], [15].

This kind of analysis bases on the weights associated to the various edges. In [8], for example, a model to evaluate weights in functional connectivity has been proposed and commented.

3. Experimental procedure

As an applicative example we consider an acoustical experiment, where two volunteers were subjected to a pleasant music and a resting state.

A similar example was treated in [23], [24]. In such papers the effect of music on the brain is considered. From [23], it comes out that regardless of the acoustical characteristic, functional brain connectivity depends on whether the music is liked or disliked. Interestingly, listening to music that is liked affects functional connectivity in regions involved in self-referential thought and memory encoding, such as the default mode network and the hippocampus. Moreover [24] reveals that music perception induces an increased synchronization of cortical regions and a more random network configuration. The differences in network architecture is not observed between musical stimuli. These findings imply that music perception leads to an emergence of a more efficient but less economical structure and requires more information processing as well as cognitive effort.

3.1. Volunteers features

...To be completed by Carlo Besta Neurological Institute

3.2. Materials

...To be completed by Carlo Besta Neurological Institute

3.3. Data recording

...To be completed by Carlo Besta Neurological Institute

3.4. Data processing

...To be completed by Carlo Besta Neurological Institute

3.5. Basal-Pleasant phase transition. Data analysis.

3.5.1. Purpose of the analysis

The purpose of our analysis was to understand if there was an emerging subgraph, common to the two volunteers, whose edges represented the connections “steadily different” during the phase transition Basal-Pleasant.

3.5.2. Processing the data

The first step in our analysis consisted in importing the available 29×2 different upper-triangular 89×89 -sized matrices $A_i^{(s)}$ as *Matlab*[®] files. In this example $s = 1, 2$, since we treat the phase transition between two phases: the Basal and the Pleasant condition. The matrices were symmetric, which allowed a better managing of the *Matlab*[®] scripts. Of course, the resulting symmetric matrices have zero entries on the main diagonal, which represents the absence of self loops in the neural brain network, meaning that nodes autocorrelation is excluded. Moreover, each entry was rounded at its fourth decimal digit.

The comparison between the two different states has been managed by computing the differences of the elements belonging to the corresponding databases. A main problem in our analysis is caused by the fact that each one of the two available databases, *Bologna* and *Abbondanza*, has no temporal correlation with the other. This means that, for a fixed index $t \in \{1, \dots, 29\}$, the matrix $A_i^{(s)}$ refers to different temporal slots for different values of s . As a consequence, a precise picture of the transition from one state to the other can be obtained by computing all the possible differences between pairs of matrices belonging to the two related databases.

We begun by focusing on the states $s = 1, 2$, namely, we investigated the transition Basal-Pleasant, represented by the matrices $A_i^{(1)} - A_j^{(2)}$, for $i, j \in \{1, \dots, 29\}$. Since the entries of each matrix can assume values in $[0, 1]$, the range of the entries of each matrix $A_i^{(1)} - A_j^{(2)}$ is the $[-1, 1]$ real interval. For a easier exposition, in the following we denote $A_i^{(1)}$ by BA_i , and $A_j^{(2)}$ by PL_j .

3.5.3. Data analysis

For any fixed temporal index $i \in \{1, \dots, 29\}$, we have computed $BA_i - PL_j$ for all $j \in \{1, \dots, 29\}$, so collecting a table as represented in Figure 2.

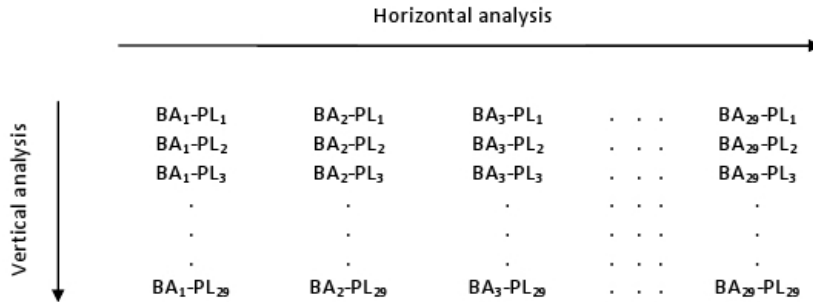


Figure 2: Vertical and horizontal analysis

This table can be explored both in the horizontal and in the vertical directions. Each column resumes the comparison of a fixed Basal temporal slot with all the 29 Pleasant temporal slots. The converse holds for the rows.

Our target was to find a characterization of the entries that more often appear in the computed differences. These represents the correlations between pairs of nodes that are more sensitive to the transition from the Basal to the Pleasant state. In particular, we looked for the entries having greater absolute values, because these denote the greater differences in correlations. Since the range of the entries is $[-1, 1]$ we are mainly interested to focus on a right neighborhood of -1 , and on a left neighborhood of $+1$, the width of these neighborhood depending on the distribution

of the entries of each matrix.

To this purpose, we organized each column in a single 89×2581 -sized matrix $C_i = [c_{hl}]_i$ ($i \in \{1, \dots, 29\}, h \in \{1, \dots, 89\}, l \in \{1, \dots, 2581\}$), obtained by connecting the rows of all the 29 matrices $BA_i - PL_j$ ($j = 1, \dots, 29$) of size 89×89 forming the column. Then we computed the distribution of the entries of such a matrix, which resulted in histograms organized in ten different bins. See for example Figure 3 for the case $C_1 = BA_1 - PL_j$, $j = 1, \dots, 29$, concerning the first column. We remark that this distribution is not Gaussian, and this can be easily checked by the Shapiro-Wilk test.

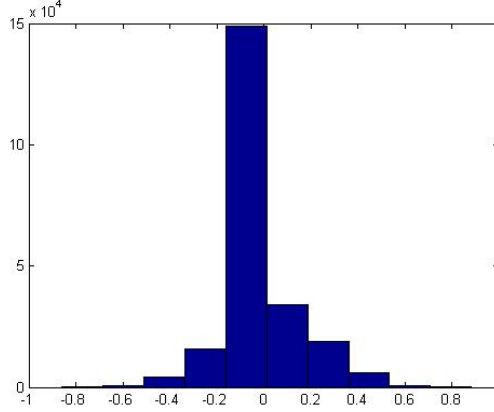


Figure 3: Histogram showing the distribution of the values of the entries of the union of the matrices $BA_1 - PL_j$, with $j = 1, \dots, 29$.

3.5.4. Thresholding procedure

For each column, we selected the center of the third bin of the corresponding histogram as the threshold $\xi_i(L)$ determining the right neighborhood of -1 . Therefore, for each $i \in \{1, \dots, 29\}$, we turned each $C_i = BA_i - PL_j$ in a thresholded binary matrix $[C_i]_L^- = [\bar{c}_{hk}^i]$ as explained in Subsection 2.1

As already mentioned, in the case $i = 1$, we have $\xi_1(L) = -0.4232$ and $\xi_1(R) = 0.4482$.

For each $i = 1, \dots, 29$, the corresponding 29 left thresholded 89×89 -sized binary matrices had been later summed up, to form a matrix $S_i(L)$ that condensed the information in the right neighborhood of -1 . Each entry of $S_i(L)$ could assume a value ranging from 0 to 29, which denoted the number of slots of 2 seconds where the corresponding pair of nodes were correlated. Analogously, we got a matrix $S_i(R)$ where the information in the left neighborhood of 1 were condensed.

From these matrices we could extract several types of graphs that could be assumed as representative of the transition Basal-Pleasant. These could be obtained by fixing new thresholds λ , corresponding to the minimum number of slots of 2 seconds that we assumed as indicative of a permanent difference between the Basal and the Pleasant states. Of course $\lambda = 29$ would have denoted an absolute permanent difference, and represented an ideal threshold. More realistically, we should relax this threshold to some intermediate value.

Following the above argument, we first computed the effective maximum M_i of each matrix $S_i(L)$ (and the same for $S_i(R)$), and later we have investigated the cases where $\lambda = M_i$, $\lambda = \frac{4}{5} M_i$, corresponding to the 80% of the slots, and $\lambda = \frac{1}{2} M_i$, namely, the 50% of the slots.

As an example let us consider thresholded matrices $[BA_1 - PL_j]_t^-$, the subscript t stands for “thresholded” while the superscript $-$ specify that the analysis focused on the right interval of -1 .

In this way, we obtained 29 binary matrices.

The next step was to sum the entries of any of these matrices so that to obtain one matrix, that we called $S_1(L)$, whose dimension was 89×89 . Figure 4 shows such a matrix. We found that the maximum value of such a matrix was 29 (we remind the reader that, *a priori*, the maximum value of such could be lesser or equal to 29).

It was also interesting to weaken the request to find an emergent subgraph throughout the 29 epochs. For example, we could be interested in finding the connection that are steadily different throughout at least the 80% of the 29 epochs (we are meaning vertical analysis).

To do this, for the first thing, it was necessary to calculate the 80% of the maximum value of the matrix $S_1(L)$, that we found to be equal to 29. The calculation gave 23.2, this value represented the searched value of the threshold. For the sake of precision we rounded down to the nearest integer, i.e. 23, this was value used in the *Matlab*[®] code ¹.

Once again we thresholded the matrix $S_1(L)$. Doing so, we obtained again a binary matrix whose entries were 0 and 1 depending if the entries of matrix $S_1(L)$, a_{kl} , $k = 1, \dots, 29$, $l = 1, \dots, 29$ where below or above 23.

With the purpose to perform a deeper analysis we searched for the emerging subgraph made up of the links steadily different at least for the 50% of the 29 epochs. The procedure was the same of that showed above.

In this case we thresholded the matrix $S_1(L)$ with a value equal to 14. In fact the 50% of the maximum value of the entries of matrix $S_1(L)$ (that we recall being 29) was 14.5 that we rounded down to 14.

Figure 4 shows matrix $S_1(L)$, every pixel is associated to a specific color.

By analyzing Figure 4 the reader could note that there is a emergent subgraph, throughout the 29 epochs, constituted by only one link. This link is the dark-red colored pixel.

Such a link represents the connection between the nodes corresponding to the *left inferior frontal gyrus, opercular part* and the *left inferior frontal gyrus, triangular part* (see the atlas in Table 1). Then, we thresholded FC matrix $S_1(L)$, so that the domain of the analysis is the 80% of the epochs (or equivalently the 80% of the maximum value of $S_1(L)$). Further, the FC matrix $S_1(L)$ was thresholded the 50% of the epochs. The process is the same of that showed for the case 80%.

In the same way we analyzed the other database (Abbondanza). If we refer to the (right) neighborhood of -1 , i.e. when the Pleasant phase prevails on the Basal phase, we obtained a general agreement with what we found in the Bologna case which confirms that specific nodes (cerebral areas) are involved. Specifically, the involved cerebral areas are part of the parietal and frontal lobe. However and importantly, the same conclusion does not hold for the (left) neighborhood of $+1$, where the Basal phase dominates the Pleasant phase. In fact, our analysis showed that it seems that there is not an emergent subgraph.

A similar analysis was performed in the neighborhood of $+1$ both for the subject *Bologna* and *Abbondanza*. The results are shown in Table 3 and Table 5.

3.6. Interpretation of the results

The analysis of the two databases Bologna and Abbondanza provides several interesting information.

In detail: First, for any subject it is possible to understand which are the most recurring links

¹This operation does make sense since the values of the entries are integers, as is the threshold in order to make homogeneous the analysis.

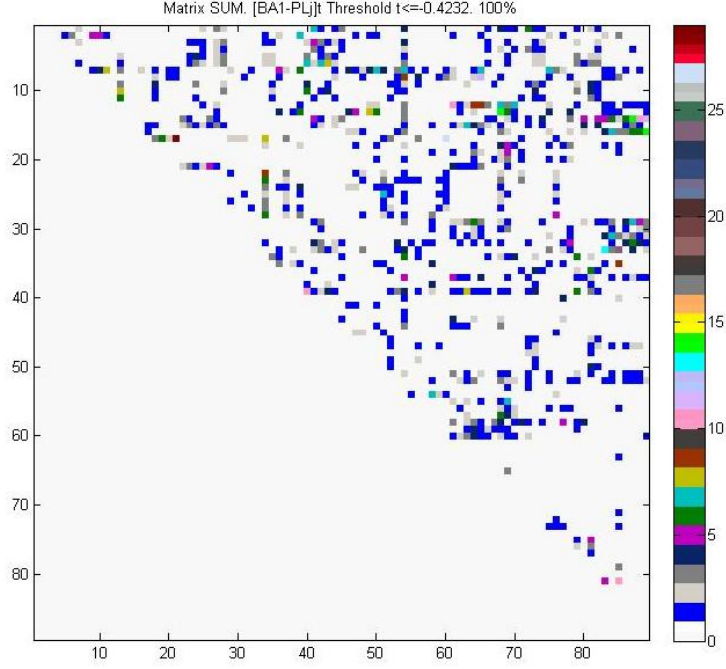


Figure 4: The example consider matrix $S_1(L)$ without a thresholding process. We remind the reader that the colors of the pixels are relative to the presence of the associated link throughout the epochs. For example the dark-red pixel represents the link always active along the 29 epochs. When the domain of analysis is 100%, i.e. matrix not λ -thresholded, there is a number of colors, each representing a value ranging from 0 to 29.

throughout all the temporal slots (horizontal analysis), the 80% and the 50% of them. The results of this analysis leads to an interpretation of a possible emerging graph.

Second, from data we pulled out further information about the links involving the “stronger” nodes. Specifically, we identified the nodes of the links involved in every temporal slot (see the red colored links in the Appendix), in other words the links that were always present in the vertical analysis (see Figure 2). These links might, or not, be connected to each other. Then, we expanded the graph theoretical analysis by identifying other links rising between that nodes and other nodes emerging after the thresholding processes (cf. Subsection 3.5.4); these links are the blue and the grey ones in temporal slots shown in the Appendix.

We apply this procedure for any subject and for the two neighborhoods -1 and $+1$. The results are shown in Figure 5(a), Figure 6(a), Figure 7(a) and Figure 8(a). It is immediate to note that the links have different thickness, this is due to the different weights associated to them. We defined a specific algorithm to calculate such a weight. In particular, we counted if a particular link was present in every single temporal slot (see Figure 2 and the Appendix), and in case, where it appeared (i.e. if was present in the range 100% (red-colored links in 6), 80% (blue-colored links) or 50% (grey-colored links)). Then we extended the process to the other temporal slots (horizontal analysis). In closing, the general formula we used to calculate the weight associated to a link connecting two nodes i and j was:

$$W_{ij} = l \cdot 1 + m \cdot 0.8 + n \cdot 0.5 \quad (2)$$

Where l is the number of temporal slots in which the link $i-j$ was present in the range 100%. This number could be zero, in this case we should count how many times the link $i-j$ was present in the range of 80%, we denoted such a number with m . If m vanished, we performed the last analysis by counting how many time the link appeared in the range 50%. We named such a number with the letter n .

For example, for the subject *Bologna*, in the analysis focusing on the neighborhood of -1 , the links $17-25$ had weight 3.2 since it was not present in any of the range 100% of the temporal slots (so $l = 0$), but it appeared in the range 80% in four different slots (so $m = 4$). Of course since it was present in the range 80% it was surely present in the range 50% , then we set $n = 0$, in order to avoid a double counting.

To carry on the Graph Theoretical Analysis we made use of different software: *Matlab*[®], *Excel*[®] and *Gephi*.

We emphasize that this kind of analysis was conceptually different from the statistical one since it is proper of the Graph Theoretical analysis.

In closing, in Section 4 we also made a comparison between the emerging subgraphs of the two subjects *Bologna* and *Abbondanza* and we suggested a common emerging subgraph.

3.6.1. Database *Bologna*: conclusions

Statistical Analysis

Let us start with the database *Bologna*. Table 2 and Table 3 give a general view about the results found after having performed the horizontal analysis over the 29 epochs: This means that we found, for each of the matrices $BA_i - PL_j$, $i = 1, \dots, 29$, $j = 1, \dots, 29$, i.e. for every temporal slot (vertical analysis), the relative subgraphs made up of the connections which were “steadily different” throughout all the 29 epochs, the 80% as well as the 50% of them.

Subgraphs analysis. Interval of -1			
Subgraph	Connections	Cerebral Areas	Presence along the 29 epochs
100%	17-21	Left inferior frontal gyrus, opercular part - Left inferior frontal gyrus, triangular part	4 times
	17-60	Left inferior frontal gyrus, opercular part - Right inferior parietal lobule	2 times
80%	17-21	Left inferior frontal gyrus, opercular part - Left inferior frontal gyrus, triangular part	14 times
	17-60	Left inferior frontal gyrus, opercular part - Right inferior parietal lobule	11 times
50%	17-21	Left inferior frontal gyrus, opercular part - Left inferior frontal gyrus, triangular part	14 times
	17-60	Left inferior frontal gyrus, opercular part - Right inferior parietal lobule	15 times

Table 2: Database *Bologna*. Analysis in the right interval of -1 . The table shows the final considerations about emerging subgraphs made up of steadily different connections in different epochs.

The link $17 - 21$ seems to be the most important when the Pleasant phase prevails on the Basal one, nevertheless, considering the horizontal analysis, it is present for nearly 50% of the epochs (14 epochs over 29).

Subgraphs analysis. Interval of $+1$			
Subgraph	Connections	Cerebral Areas	Presence along the 29 epochs
100%			
80%	17-22	Left inferior frontal gyrus, opercular part - Right inferior frontal gyrus, triangular part	14 times
	17-60	Left inferior frontal gyrus, opercular part - Right inferior frontal gyrus, triangular part	7 times
50%	17-22	Left inferior frontal gyrus, opercular part - Right inferior frontal gyrus, triangular part	14 times

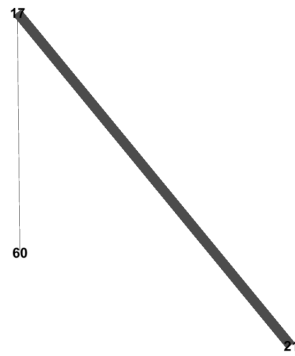
Table 3: Database *Bologna*. Analysis in the left interval of $+1$. Final considerations about emerging subgraphs made up of steadily different connections in different epochs. Note that there is not any link always active in every temporal slot.

In this analysis, definitely, there is not a clearly emerging subgraph since there is not a link that could be a sort of “strong candidate” to be considered a component of the emerging subgraph. The only link of a certain interest is $17 - 22$, but it exhibit itself only if we focus on the range 80% . However, it does not seem to have great dominance, after performing the horizontal analysis, since it is present in 14 epochs over 29 (horizontal analysis).

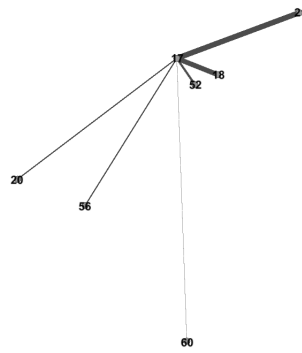
Graph Theoretical Analysis

Another results concerns the existence of an emerging graph by considering the links of the

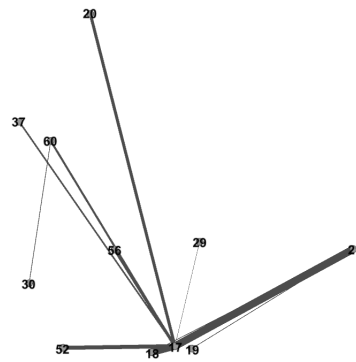
most involved nodes. Figure 5 and Figure 8 show, respectively, the emerging subgraphs in the neighborhood of -1 and $+1$ for the 100% and 80% of the epochs.



(a) 100%

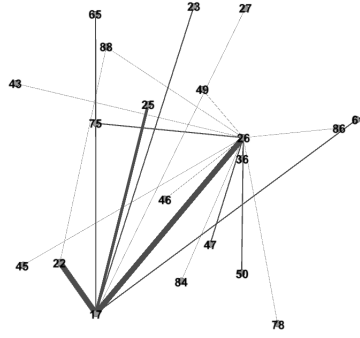


(b) 80%



(c) 50%

Figure 5: Emerging subgraphs for the subject Bologna when the Pleasant phase is dominant on the Basal phase.



(a) 80%

Figure 6: Emerging subgraph for the subject Bologna when the Basal phase is dominant on the Pleasant phase. Note that it does not exist an emerging subgraph made up by links always active. Moreover, it does not exist even an emerging subgraph in the case 50% since what we got it was a strongly connected graph, so this case is outside of our purpose (we looked for subgraphs made up by a relative small number of links).

3.6.2. The database *Abbondanza*: conclusions

Table 4 and Table 5 show the results coming from the analysis of each of the matrices $BA_i - PL_j$, $i = 1, \dots, 29$, $j = 1, \dots, 29$. We recall that the relative subgraphs are made up of the connections “steadily different” throughout all the 29 epochs, the 80% as well as the 50% of them.

Subgraphs analysis. Interval of -1			
Subgraph	Connections	Cerebral Areas	Presence along the 29 epochs
100%	13-52	Left Posterior cingulum - Left globus pallidus	11 times
	16-18	Right Cuneus - Right inferior frontal gyrus, opercular part	12 times
	82-88	Right middle temporal gyrus - Right superior temporal gyrus	7 times
80%	13-52	Left Posterior cingulum - Left globus pallidus	16 times
	16-18	Right Cuneus - Right inferior frontal gyrus, opercular part	22 times
	82-88	Right middle temporal gyrus - Right superior temporal gyrus	17 times
50%	13-52	Left Posterior cingulum - Left globus pallidus	22 times
	16-18	Right Cuneus - Right inferior frontal gyrus, opercular part	23 times
	82-88	Right middle temporal gyrus - Right superior temporal gyrus	20 times

Table 4: Database *Abbondanza*. Analysis in the right interval of -1 . Final considerations about emerging subgraphs made up of steadily different connections in different epochs.

In brief, in the right interval of -1 , we conclude that there is an emerging subgraph. The links more interesting seem to be the connection between node 16 and 18, between 13 and 52 and between 82 and 88. They appear more often in comparison to other links.

Subgraphs analysis. Interval of $+1$			
Subgraph	Connections	Cerebral Areas	Presence along the 29 epochs
100%	1-88	Left Amygdala - Right superior temporal gyrus	3 times
80%	1-88	Left Amygdala - Right superior temporal gyrus	12 times
	2-88	Right Amygdala - Right superior temporal gyrus	17 times
	85-88	Left superior temporal pole - Right superior temporal gyrus	14 times
50%	1-88	Left Amygdala - Right superior temporal gyrus	20 times
	2-88	Right Amygdala - Right superior temporal gyrus	22 times
	85-88	Left superior temporal pole - Right superior temporal gyrus	21 times

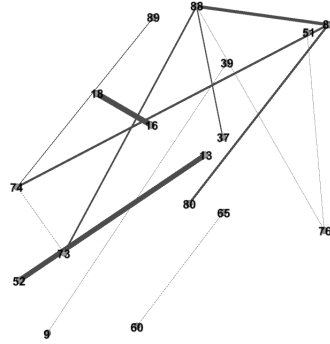
Table 5: Database *Abbondanza*. Analysis in the left interval of $+1$. Final considerations about emerging subgraphs made up of steadily different connections in different epochs.

We conclude that there is not a subgraph always active, but, remarkably the node 88, asso-

ciated with the right superior temporal gyrus, is strongly involved. It links with Amygdala and temporal lobe. And this is not unexpected for an acoustical test.

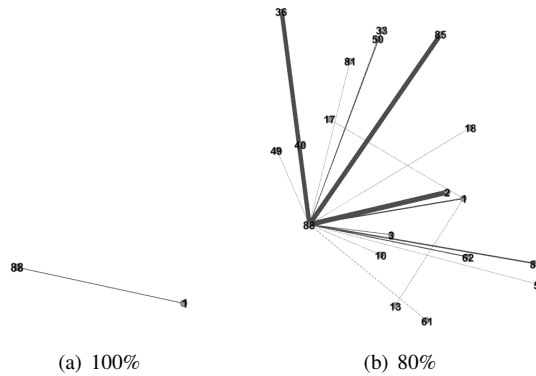
Graph Theoretical Analysis

The Graph Theoretical analysis leads to the following results:



(a) 100%

Figure 7: Emerging subgraphs for the subject Bologna when the Pleasant phase is dominant on the Basal phase. The subgraph corresponding to the links always active is composed by a significative high number of links. Hence, there is no need to expand the analysis to the 80% and 50%.



(a) 100%

(b) 80%

Figure 8: Emerging subgraph for the subject Bologna when the Basal phase is dominant on the Pleasant phase. The case 50% is not showed due to the huge number of links composing the graph, in this case, and for our aims, it does not make sense call it subgraph.

4. Results

We are aware that an analysis on two subjects cannot lead to definitive conclusions. Nevertheless, by comparing the analysis of the neighborhood of -1 , our results seem to show that the emerging graph involves cerebral areas that are not generally concerned with the acoustic process, such as the primary auditory cortex². In fact by observing at glance Figure 9 the nodes are

²We recall that the primary auditory cortex is the part of the temporal lobe, such cortex processes auditory information (both in humans and in animals). In humans, the primary auditory cortex is located on the superior temporal plane, within the lateral fissure and comprising parts of Heschl's gyrus and the superior temporal gyrus, including planum polare and planum temporale (roughly Brodmann areas 41, 42, and partially 22).

60, the right inferior parietal lobule, 17 and 18, respectively, the left and inferior frontal gyrus, opercular part. This remarks that the functional connectivity affects cerebral areas associated to different tasks.

Hence, this leads to concluding that in acoustical experiments it is advisable focusing not only on areas traditionally associated with acoustic process.

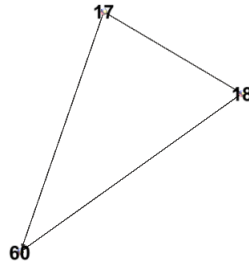


Figure 9: From the graph theoretical analysis of the data of the two subjects Bologna and Abbondanza it seems that a possible subgraph could be composed by nodes 60, 18 and 17. This nodes represent areas that are not directly associated to the auditory process

Regarding the neighborhood of +1, i.e. when the Basal phase dominates on the Pleasant phase, the graph theoretical analysis does not seem to provide a clear emerging subgraph. However, the analysis shows how the temporal lobe, specifically the right superior temporal gyrus (node 88) plays a prominent role both in the subject *Bologna* and in *Abbondanza*. We might guess that this node could link with other nodes belonging to the limbic system, but as far as we got we have not enough evidence to support our speculation (if one on hand it could be advisable push the analysis forward by means of the analysis of weaker connections, on the other this action would turn us away from our purpose, that is find a subgraph made up by a small number of edges representing the connections steadily different throughout the length of the experiment.

The neighborhood of -1 corresponds to the links mainly stimulated, with respect to the Basal phase (to be interpreted as the baseline), from musical test. Conversely, the neighborhood of +1 matches to the links “less sensitive” to the test run.

In [23], [24] it was shown that in an acoustical experiment the cerebral regions involved are not only the ones engaged in the acoustical process but also others, that generally are not interested in such a process. Our graph analysis, despite of the small number of subjects undergoing the experiment, seem to agree with these results.

If we wish to find a phrase that could summary our results, it would be declaimed in such a way: “pleasant music tends to create links more than to destroy them.”

5. Conclusions

In this paper, we have proposed a methodology to manage neurobiological datasets. Such a methodology could be applied to data of different nature such as EEG/MEG, fMRI, PET or a coupling of an electrophysiologic measurement technique with a hemodynamic one.

The thresholding procedure has been described, both for the binarization steps and for the subsequent graph representation of the regions of interest. The rule of assigning edge weights has been also detailed.

We provided an example of application of our method by treating MEG data generated in acoustical experiments, where pleasantness and resting state are involved.

We observed the changes in functional connectivity from a Basal condition, which is essentially a resting state condition, to a Pleasant condition, where the volunteers listened to music that they classified as agreeable.

We focused on the existence of links (generally not known *a priori*) steadily different, that is connections which are always different throughout the experiment duration.

There are other typologies of acoustical analysis or different tasks of analysis that could be performed by making use of the methodology shown in this paper. For example one could be interested in determining the existence of an emerging subgraph made up of links invariant all along the time of the experiment, when one or more subjects undergo musical and silent stimuli. In other words, the goal is to find the links always equal throughout the temporal slots.

Moreover, by performing a neurobiological experiment with a significative number of subjects, it could be possible to carry out a deeper network analysis with the purpose of detecting the existence of motifs [21] or leading a clustering analysis to understand the existence of provincial, central hubs and modules [7], [19], [20], [22].

Such a methodology of graph representation of database comparison could be useful to highlight cerebral connections that generally are not expected, also in view of identifying possible regions responsible for psychiatric disorders [2], [3], [10] as well as to assess how tasks of different nature (musical, cognitive, decisional-making, etc.) affect the functional connectivity of the brain.

References

- [1] AGOSTA, F. ET AL. (2013) Brain network connectivity assessed using graph theory in frontotemporal dementia. *Neurology* 81, 134143
- [2] BASSETT, BULLMORE, VERCHINSKI, MATTAY, WEINBERGER, MEYER-LINDENBERG (2008) Hierarchical Organization of Human Cortical Networks in Health and Schizophrenia. *The Journal of Neuroscience*, 10 September 2008, 28(37): 9239-9248;
- [3] BASSETT, D.S. AND BULLMORE, E.T. (2009) Human brain networks in health and disease. *Curr. Opin. Neurol.* 22, 340347
- [4] Bullmore ET, Bassett DS. 2011. Brain graphs: graphical models of the human brain connectome. *Annu Rev Clin Psychol.* 7:113–140.
- [5] BOLLOBÁS B. (1985) *Random graphs*. London: Academic.
- [6] BULLMORE AND SPORN (2009) Complex Brain Networks Graph Theoretical Analysis Of Structural and Functional Systems. *Nature Reviews Neuroscience* 10, 186-198 (March 2009) — doi:10.1038/nrn2575
- [7] CROSSLEY, N. A., MECHELLI, A., SCOTT, J., CARLETTI, F., FOX, P. T., MCGUIRE, P., BULLMORE, E. T. (2014) The hubs of the human connectome are generally implicated in the anatomy of brain disorders. *Brain* 1372382-2395.
- [8] FINOTELLI, P., DULIO, P. A Mathematical Model for Evaluating the Functional Connectivity Strongness in Healthy People. (2015). Submitted 2nd round to Archives Italiennes de Biologie.
- [9] FINOTELLI, P., DULIO, P. Graph Theoretical Analysis of Brain. An Overview. (2015). Published in *Scienze e Ricerche* n. 9, July 2015, pp. 89-96.
- [10] FORNITO, A. et al. (2012) Schizophrenia, neuroimaging and connectomics. *Neuroimage* 62, 22962314.
- [11] FORNITO, A., ZALESKY, A., BREAKSPEAR, M. (2015). The connectomics of brain disorders. *Nature Reviews Neuroscience* 16, 159172 (2015) doi:10.1038/nrn3901
- [12] Friston, K.J., Frith, C.D., Liddle, P.F., Frackowiak, R.S.J. (1993). Functional connectivity: the principal component analysis of large (PET) data sets. *J. Cereb. Blood Flow Metab.* 13, 514.
- [13] FRISTON, K.J. (1994). Functional and Effective Connectivity in Neuroimaging: A Synthesis. *Human Brain Mapping* 2:56-78(1994). 273:503511.
- [14] KAISER M. (2011). A tutorial in connectome analysis: topological and spatial features of brain networks. *Neuroimage.* 57:892–907.

- [15] (2015). Identifying patients with Alzheimer’s disease using resting-state fMRI and graph theory. Clin Neurophysiol. 2015 Apr 1. pii: S1388-2457(15)00224-2. doi: 10.1016/j.clinph.2015.02.060.
- [16] RUBINOV M., SPORNS O. (2010). Complex network measures of brain connectivity: uses and interpretations. Neuroimage 52(3):1059-69.
- [17] RUTTER ET AL. (2013) Graph theoretical analysis of resting magnetoencephalographic functional connectivity networks. Front Comput Neurosci. 2013 Jul 12;7:93. doi: 10.3389/fncom.2013.00093. eCollection 2013.
- [18] SALVADOR R., SUCKLING J., SCHWARZBAUER C., BULLMORE E. (2005), Undirected graphs of frequency-dependent functional connectivity in whole brain networks. Philos Trans R Soc Lond B Biol Sci 360(1457):937-46.
- [19] SPORNS, O. Networks of the Brain. MIT Press. 2010.
- [20] SPORNS, O., HONEY, C. J., AND KÖTTER, R. “Identification and classification of hubs in brain networks” PLoS ONE, vol. 2, no. 10, Article ID e1049, 2007.
- [21] SPORNS, O., KÖTTER, R. Motifs in Brain Networks. PLoS Biol 2(11): e369. doi:10.1371/journal.pbio.0020369. Academic Editor: Karl J.
- [22] VAN DEN HEUVEL AND OLAF SPORNS (2013) Network hubs in the human brain. Trends Cogn Sci. 2013 Dec;17(12):683-96. doi: 10.1016/j.tics.2013.09.012.
- [23] WILKINS, R. W., HODGES, D. A., LAURIENTI, P. J., STEEN, M. & BURDETTE, J. H. (2014). Network science and the effects of music preference on functional brain connectivity: from Beethoven to Eminem. Sci Rep. Sci Rep 2014 28;4:6130. Epub 2014.
- [24] WU, J., ZHANG, J., DING, X., LI, R., ZHOU, C. (2013). The effects of music on brain functional networks: A network analysis. Neuroscience 250, 4959 (2013) 12.

6. Appendix

6.1. Example of results. Case: Bologna, neighborhood of -1

As an example we show in the following the results of our (vertical) analyzes for the subject *Bologna* in the neighborhood of -1 for every temporal slot (i.e. the case when the Pleasant phase dominates on the Basal phase). The connections in red are those always present in every vertical slots (see Figure 2, in blue those present in the 80% of the epochs and in grey those present in the 50% of the epochs). We remark that all the vertical temporal slots contribute to define the horizontal analysis.

The reader interested in the other data feels free to write to the corresponding author.

SLOT 1	34 70	26 27	82 85	23 64	7 76
17 21	39 43	32 39	SLOT 6	29 51	2 44
17 21	48 53	SLOT 5	17 52	29 52	2 82
17 60	73 81	17 20	22 24	40 44	7 12
33 85	SLOT 3	33 89	43 44	40 45	7 13
13 68	17 21	41 85	1 44	43 44	7 37
14 87	17 60	41 89	4 44	SLOT 7	7 46
16 89	17 21	79 85	7 39	17 21	7 50
17 21	17 60	81 85	12 29	17 21	7 51
17 52	17 21	81 89	12 65	17 60	7 76
17 60	17 60	14 87	13 29	8 87	8 12
33 85	SLOT 4	14 89	13 65	17 21	8 13
SLOT 2	17 21	17 20	15 51	17 60	14 83
14 89	17 60	28 85	16 61	21 38	41 74
17 18	17 21	33 85	17 18	21 77	41 82
17 21	17 60	33 89	17 20	40 87	42 74
17 60	3 32	41 85	17 52	42 85	42 82
14 87	14 83	41 88	17 60	46 52	45 74
14 89	17 18	41 89	22 24	52 77	SLOT 9
17 18	17 21	45 85	22 25	55 58	17 21
17 20	17 56	79 83	22 27	60 77	11 51
17 21	17 60	79 85	22 61	SLOT 8	14 84
17 60	22 27	81 85	22 64	7 12	14 89
33 73	22 64	81 89	23 27	7 51	17 21

50 51	80 84	44 58	14 48	SLOT 15	7 9
3 13	SLOT 11	44 59	14 49	14 89	7 10
7 10	2 85	46 60	14 50	17 21	7 75
9 29	7 11	48 73	14 75	70 72	9 12
9 30	7 46	49 73	14 83	14 86	9 13
10 12	7 50	52 54	14 84	14 87	9 14
10 29	8 85	56 58	14 85	14 88	9 19
10 37	17 21	SLOT 12	14 89	14 89	9 51
10 47	1 53	17 21	15 51	17 20	10 50
10 51	2 84	17 21	16 83	17 21	14 38
10 76	2 85	17 60	16 89	17 60	14 75
11 12	2 87	2 85	17 20	28 85	14 83
11 37	7 10	15 32	39 46	35 85	14 84
11 51	7 11	17 20	39 50	70 72	14 85
11 76	7 36	17 21	39 51	79 85	14 87
12 50	7 46	17 60	39 52	SLOT 16	14 89
14 49	7 50	29 32	39 76	7 11	15 18
14 83	7 51	30 32	72 85	7 50	15 19
14 84	7 75	SLOT 13	78 85	7 75	15 38
14 86	7 76	9 11	SLOT 14	17 20	17 18
14 88	8 85	9 36	14 83	17 21	17 19
14 89	9 18	9 37	16 30	17 52	17 20
17 21	12 28	12 39	17 18	17 56	18 29
17 60	14 38	14 75	17 21	17 60	33 85
30 39	15 20	14 83	17 60	7 10	38 39
36 51	16 38	14 85	49 84	7 11	45 74
37 50	16 77	39 46	49 86	7 36	48 53
37 89	17 19	39 51	14 83	7 49	48 55
39 76	17 21	4 9	14 84	7 50	53 57
46 51	17 29	4 10	14 87	7 75	54 57
50 51	17 37	6 76	14 89	9 12	54 59
51 75	17 52	8 35	15 19	9 32	57 68
SLOT 10	20 55	8 79	15 31	9 52	59 68
14 87	25 41	8 81	15 32	10 13	SLOT 18
17 21	26 38	8 85	16 19	10 32	1 40
7 84	27 35	8 87	16 30	15 32	3 12
13 25	27 41	9 11	17 18	17 20	4 40
14 87	27 73	9 14	17 20	17 21	7 11
14 89	27 79	9 36	17 21	17 37	7 39
15 20	27 81	9 37	17 52	17 52	7 50
16 47	29 53	9 50	17 56	17 56	11 12
17 21	33 85	9 51	17 60	17 60	11 51
17 60	38 82	9 75	19 30	19 56	12 46
19 56	39 60	9 76	20 30	32 39	12 47
20 30	40 55	10 11	29 31	35 39	12 50
20 31	41 58	10 36	31 32	SLOT 17	16 51
37 89	41 85	10 37	32 39	5 39	37 47
48 88	42 57	10 46	37 89	6 39	37 48
48 89	42 69	10 50	46 84	14 83	39 51
49 73	42 85	10 75	47 84	14 84	46 51
49 88	43 52	11 39	49 84	17 18	50 51
49 89	43 60	12 39	49 86	5 39	1 12
54 59	43 87	13 39	49 88	6 9	1 13
77 80	44 57	14 36	49 89	6 39	1 40

1 42	13 29	29 46	2 87	7 76	33 39
1 52	14 83	29 50	7 9	72 85	35 39
1 53	14 84	29 51	7 10	79 85	39 52
2 43	14 85	29 52	7 15	79 89	55 68
3 12	14 87	29 76	7 39	84 89	56 58
3 40	14 88	29 88	8 72	3 7	1 55
3 53	14 89	39 53	8 85	3 40	1 59
4 40	15 37	39 77	13 25	3 43	2 5
4 55	15 76	54 82	13 66	4 6	2 6
5 43	17 18	74 85	14 72	5 40	2 39
5 51	17 19	SLOT 21	14 78	5 43	3 42
6 43	17 20	17 21	14 83	6 40	3 44
6 51	19 37	17 21	14 89	6 42	3 52
7 11	29 51	17 60	17 18	6 43	3 53
7 39	29 52	2 72	17 20	7 37	4 44
7 46	29 76	2 78	17 52	7 47	4 55
7 50	SLOT 20	2 85	17 56	7 49	5 13
9 37	11 13	8 85	17 60	7 51	5 52
9 51	17 21	14 30	18 21	7 76	5 53
10 37	17 60	14 87	19 24	14 83	6 13
10 43	1 15	14 89	28 34	14 87	6 42
10 51	1 29	15 19	33 69	14 89	6 44
10 76	7 11	17 18	33 72	17 18	6 52
11 12	7 39	17 20	33 78	28 87	6 53
11 51	7 46	17 21	34 35	35 85	8 58
12 36	7 47	17 52	40 72	35 89	10 52
12 46	7 48	17 60	43 72	36 38	10 53
12 47	7 49	33 72	51 65	36 76	12 59
12 48	7 50	35 72	66 71	36 77	12 68
12 49	9 40	35 78	78 81	38 48	13 39
12 50	9 53	41 72	SLOT 23	38 84	13 58
13 76	11 13	41 78	14 89	39 43	13 68
16 51	12 39	41 85	48 88	50 76	17 20
18 30	12 61	44 72	49 88	72 83	17 31
19 20	12 65	45 72	57 58	72 85	18 24
20 29	13 15	45 78	7 10	72 89	23 34
36 37	13 29	72 79	14 88	73 85	28 39
36 51	13 36	72 81	14 89	75 76	33 39
37 39	13 39	72 87	17 18	75 77	35 39
37 47	13 46	75 82	47 88	77 84	38 52
37 48	13 50	78 79	48 86	78 85	38 56
37 49	13 61	78 81	48 88	78 89	39 40
39 51	13 64	SLOT 22	49 88	79 83	39 43
39 76	13 65	2 72	49 89	79 85	39 52
46 51	15 51	7 9	56 58	79 89	39 79
46 53	15 76	7 10	57 58	81 85	52 77
47 51	17 18	7 39	58 59	81 89	54 55
50 51	17 20	8 85	SLOT 24	84 89	54 57
51 75	17 21	17 18	3 43	SLOT 25	55 59
SLOT 19	17 37	17 56	5 43	1 55	55 68
13 29	17 52	17 60	6 40	4 44	56 58
14 83	17 56	2 72	6 43	6 52	58 60
14 89	17 60	2 78	7 47	10 52	SLOT 26
12 29	19 52	2 85	7 51	12 59	7 39

14 38	17 52	39 47	79 85
14 77	17 56	41 66	81 85
17 18	18 19	41 85	
40 51	18 30	43 72	
2 43	22 27	44 56	
5 12	39 47	45 85	
5 51	41 85	72 85	
7 9	72 85	78 85	
7 11	81 85	81 85	
7 13	2 59	SLOT 29	
7 36	2 67	2 85	
7 39	2 74	7 11	
7 75	2 82	7 36	
12 40	2 83	7 46	
14 38	2 84	7 47	
14 48	2 85	7 50	
14 77	2 86	7 75	
14 89	2 88	17 18	
17 18	7 48	17 20	
40 51	9 47	17 52	
41 43	10 48	23 24	
69 78	12 61	41 85	
SLOT 27	12 65	79 85	
45 82	13 20	2 85	
49 88	13 41	7 9	
74 86	15 16	7 11	
82 84	15 18	7 36	
82 86	16 30	7 39	
10 29	16 31	7 46	
10 37	17 18	7 47	
10 51	17 20	7 48	
10 76	17 37	7 49	
14 38	17 52	7 50	
18 56	17 56	7 75	
36 38	17 60	14 78	
36 77	18 19	14 86	
38 75	18 29	14 87	
39 51	18 30	14 88	
45 74	18 31	14 89	
45 82	18 56	17 18	
45 88	19 21	17 20	
49 88	20 25	17 52	
73 74	20 52	17 60	
73 85	22 24	23 24	
74 84	22 27	28 83	
74 86	22 66	28 85	
75 77	23 34	28 87	
75 89	27 33	35 85	
80 86	27 41	36 72	
82 84	29 49	40 85	
82 86	29 65	41 85	
SLOT 28	30 60	42 85	
2 85	33 85	56 58	
2 88	34 44	79 83	